Northumbria Research Link

Citation: Jin, Yidan, Jiao, Shuo, Dolfing, Jan and Lu, Yahai (2021) Thermodynamics shapes the biogeography of propionate-oxidizing syntrophs in paddy field soils. Environmental Microbiology Reports, 13 (5). pp. 684-695. ISSN 1758-2229

Published by: Wiley-Blackwell

URL: https://doi.org/10.1111/1758-2229.12981 <https://doi.org/10.1111/1758-2229.12981>

This version was downloaded from Northumbria Research Link: http://nrl.northumbria.ac.uk/id/eprint/46434/

Northumbria University has developed Northumbria Research Link (NRL) to enable users to access the University's research output. Copyright © and moral rights for items on NRL are retained by the individual author(s) and/or other copyright owners. Single copies of full items can be reproduced, displayed or performed, and given to third parties in any format or medium for personal research or study, educational, or not-for-profit purposes without prior permission or charge, provided the authors, title and full bibliographic details are given, as well as a hyperlink and/or URL to the original metadata page. The content must not be changed in any way. Full items must not be sold commercially in any format or medium without formal permission of the copyright holder. The full policy is available online: http://nrl.northumbria.ac.uk/policies.html

This document may differ from the final, published version of the research and has been made available online in accordance with publisher policies. To read and/or cite from the published version of the research, please visit the publisher's website (a subscription may be required.)

Northumbria University NEWCASTLE

University Library

environmental microbiology
environmental microbiology reports

Thermodynamics shapes the biogeography of propionate-oxidizing syntrophs in paddy field soils

Journal:	*Environmental Microbiology and Environmental Microbiology Reports*
Manuscript ID	EMIR-2021-0816
Journal:	Environmental Microbiology Reports
Manuscript Type:	EMIR - Brief report
Date Submitted by the Author:	17-May-2021
Complete List of Authors:	Jin, Yidan; Peking University Jiao, Shuo; Northwest Agriculture and Forestry University Dolfing, Jan; Northumbria University Lu, Yahai; Peking University, College of Urban and Environmental Sciences
Keywords:	Rare biosphere, Propionate syntrophs, Biogeography, Methanogenesis, Paddy soil

SCHOLARONE™
Manuscripts

Thermodynamics Shapes the Biogeography of Propionate-Oxidizing Syntrophs in Paddy Field Soils

Running title: Biogeography of Propionate-Oxidizing Syntrophs

Yidan Jin,[1] Shuo Jiao,[1, 2] Jan Dolfing,[3] Yahai Lu[1*]

[1]College of Urban and Environmental Sciences, Peking University, Beijing, 100871, China

[2]Present address: State Key Laboratory of Crop Stress Biology in Arid Areas, College of Life Sciences, Northwest A&F University, Yangling, Shaanxi, 712100, China

[3]Faculty of Engineering and Environment, Northumbria University, Newcastle-upon-Tyne, NE1 8QH, England, UK

*Corresponding author: luyh@pku.edu.cn; Tel., +86 10 62750669; Fax, +86 10 62750669.

Competing interests: The authors declare that they have no competing interests.

For Peer Review Only

Summary

Soil biogeochemical processes are not only gauged by the dominant taxa in the microbiome but also depend on the critical functions of its "rare biosphere" members. Here we evaluated the biogeographical pattern of "rare biosphere" propionate-oxidizing syntrophs in 113 paddy soil samples collected across China. The relative abundance, activity and growth potential of propionate-oxidizing syntrophs were analyzed through sequencing bacterial 16S rRNA genes and anaerobic incubations to provide a panoramic view of syntroph biogeographical distribution at the continental scale. The relative abundances of four syntroph genera, *Syntrophobacter*, *Pelotomaculum*, *Smithella* and *Syntrophomonas* were significantly greater at the warm low latitudes than at the cool high latitudes. Correspondingly, propionate degradation was faster in the low latitude soils compared with the high latitude soils. The low rate of propionate degradation in the high latitude soils resulted in a greater increase of the total syntroph relative abundance, probably due to their initial low relative abundances and the longer incubation time for propionate consumption. The mean annual temperature (MAT) is the most important factor shaping the biogeographical pattern of propionate-oxidizing syntrophs, with the next factor being the soil's total sulfur content (TS). We suggest that the effect of MAT is related to the thermodynamic conditions, in which the endergonic constraint of propionate oxidation is leveraged with the increase of MAT. The TS effect is likely due to the ability of some propionate syntrophs to facultatively perform sulfate respiration.

Keywords: Rare biosphere, Propionate syntrophs, Biogeography, Methanogenesis, Paddy soil.

For Peer Review Only

Introduction

The soil microbiome plays a vital role in regulating global biogeochemistry. It has been recently documented that in spite of the immense biodiversity of the soil microbiome, only a few hundreds of phylotypes are prevalent across global soils and that these dominant phylotypes display distinct biogeographical distribution according to their habitat preferences (Delgado-Baquerizo et al., 2018). The factors shaping the biogeographic patterns of the global soil microbiome include climatic factors, edaphic properties and biological interactions (Garbeva et al., 2004; Schlatter et al., 2015; Bahram et al., 2018; Rillig et al., 2019; Steidinger et al., 2019). Identification of soil dominant taxa, their geographical distributions and the controlling factors provides a "priority" list for cultivation and genomic scrutiny that shall help in decoding biogeochemical mechanisms and pave a way toward developing global Earth system models that are soil context-dependent (Delgado-Baquerizo et al., 2018; Crowther et al., 2019; van den Hoogen et al., 2019). The dominants-focused approaches, however, will inevitably overlook the function of "rare biosphere" specialists (Lynch and Neufeld, 2015). It has been understood that biogeochemical processes are not only gauged by dominant taxa that dictate biomass turnover but also depend on critical functions of specialist members (Crowther et al., 2019). A typical example is microbial syntrophs, which play a critical role in anaerobic decomposition of organic matter and methanogenesis but have only a low relative abundance in natural environments like paddy field soils (Lueders et al., 2004; Gan et al., 2012).

Complex organic matter in anoxic environments is degraded by an anaerobic food chain comprising primary and secondary fermenters, homoacetogens and methanogens (Glissmann et al., 2001; Stams and Plugge, 2009). Polymers are initially converted to

For Peer Review Only

oligomers and monomers and subsequently fermented to short-chain fatty acids (SCFAs), alcohols, acetate, and so on. A series of SCFAs and alcohols are transiently accumulated as intermediate products during the process (Glissmann and Conrad, 2000; Glissmann et al., 2001; Rui et al., 2009; Noll et al., 2010). Therefore during the anaerobic decomposition of complex organic matter, a quite portion of the carbon flows through the SCFAs, which are subsequently degraded to acetate and CO_2 by secondary fermenters (i.e. the syntrophs) (Schink, 1997; Schink and Stams, 2006; McInerney et al., 2009; Stams and Plugge, 2009). Propionic acid, one of the major SCFAs, accounts for up to 30% of the total CH_4 formation in paddy soils (Krylova et al., 1997; Glissmann and Conrad, 2000). The process of propionate degradation is thermodynamically more constrained than that of ethanol and butyrate, making propionate degraders being slower in growth and more sensitive to environmental conditions (Schink, 1997; Boe et al., 2010; Mueller et al., 2010; Hidalgo-Ahumada et al., 2018). Identifying propionate-oxidizing key taxa and delineating their biogeographical distribution are therefore important for better understanding and predicting organic matter decomposition and carbon cycling in anoxic environments including natural wetlands and paddy field soils.

All known propionate-oxidizing syntrophs had in pure cultures so far fall into four bacterial genera: *Syntrophobacter*, *Pelotomaculum*, *Smithella* and *Desulfotomaculum* (Sieber et al., 2012; Hidalgo-Ahumada et al., 2018; Dyksma and Gallert, 2019). Their importance in anoxic environments, such as paddy field soils and natural wetlands, has been demonstrated by using various approaches such as enrichment cultivation, DNA/RNA stable isotope probing and meta-omics technology (Lueders et al., 2004; Li et al., 2015; Tveit et al., 2015; Peng et al., 2018; Xia et al., 2019). Recently, a few candidate taxa (e.g. *Ca. Syntrophosphaera thermopropionivorans* from the phylum *Cloacimonetes*,

For Peer Review Only

Ca. Syntrophopropionicum ammoniitolerans from the family *Peptococcaceae* and member from the family *Desulfobulbaceae*) were proposed to be capable of performing syntrophic propionate metabolism (Dyksma and Gallert, 2019; Singh et al., 2021). The ecophysiology and environmental significance of these organisms however have remained unclear.

Paddy field soils are human-managed ecosystems and are important contributors to global CH_4 emissions (Thauer, 1998; Conrad, 2009). About 90% of paddy fields are located in Asia with 20% of that in China (Haefele et al., 2014). Rice production in China is dominated by irrigated systems, which are distributed mainly in the lowland of eastern China, extending from the warm sub-tropics at 18°N latitude to the cool temperate regions at 50°N (Deng et al., 2019). The long history of rice cultivation makes the region an ideal site for microbial biogeography investigations that are independent of large scale variations in vegetation and soil type. In the present study, we collected 113 paddy field soils from different sites across eastern China covering a latitudinal distance of 3689 kilometers. The potential for propionate degradation in each soil was evaluated through anaerobic incubations in the laboratory. The composition and relative abundance of four known genera of propionate oxidizing syntrophs in original soils and soil samples after anaerobic incubations were investigated using high throughput sequencing of bacterial 16S rRNA genes. We show here that temperature and the total sulfur content in soil are the most important factors shaping the biogeographic distribution and functional potential of propionate-oxidizing syntrophs in paddy field soils at the continental scale.

Results and Discussion

For Peer Review Only

Biogeographical distribution of propionate syntrophs

A total of 6204541 high quality sequences of V3-V4 regions of the bacterial 16S rRNA genes were obtained from 113 paddy soil samples, which were clustered into 27411 OTUs. The most dominant OTUs were affiliated to *Proteobacteria*, *Firmicutes*, *Actinobacteria*, *Chloroflexi*, *Acidobacteria*, *Nitrospirae* and *Gemmatimonadetes* (Fig. S1). For the present study we focused on four genera of propionate-oxidizing syntrophs (i.e. *Syntrophobacter*, *Pelotomaculum*, *Smithella* and *Desulfotomaculum*) and *Syntrophomonas* (Fig. S2). A total of 30 OTUs belonging to these five syntroph genera were obtained. Members of the genus *Syntrophomonas* are not known to oxidize propionate but butyrate and fatty acids up to C_{10} (Zhang et al., 2004). The inclusion of *Syntrophomonas* in our analysis was due to the fact that *Smithella*, which utilize the C_6 dismutation pathway [$2CH_3CH_2COO^- \rightarrow CH_3COO^- + CH_3CH_2CH_2COO^-$], can release butyrate as an intermediate product, which is then metabolized by *Syntrophomonas* (Xia et al., 2019). *Desulfotomaculum* was included, even though their relative abundances were very low (Fig. S2, 3), because some *Desulfotomaculum* species such as *D. thermobenzoicum* and *D. thermocisternum* have been known to utilize propionate in coculture with methanogens (Nilsen et al., 1996; Plugge et al., 2002) and because *Pelotomaculum* species are phylogenetically a branch of *Desulfotomaculum* (Imachi et al., 2006; Imachi et al., 2007).

The total relative abundance of the five syntroph genera in combination, referred to as synTotal, ranged from 0.01 to 0.34% across 113 soil samples. This low relative abundance certificates that syntrophs in paddy soils belong to a subset of the "rare biosphere" community (defined as individual species or OTUs accounting for <0.1% of the total relative abundance). Albeit "rare" in relative abundance, the synTotal displayed

For Peer Review Only

144 a distinct geographical distribution, showing the highest relative abundance in the warm
145 low latitude soils and gradually decreasing towards the high latitude regions (Fig. 1A).
146 Conventionally the geographical division separating China into the south (low latitude)
147 and the north (high latitude) regions follows to the Qinling Mountains-Huaihe River Line
148 (latitude ≈ 32°), a critical geographical boundary for climate, landform and soil
149 conditions (Qi et al., 2016). We summarized our soil samples accordingly into a low
150 latitude and the a high latitude group, respectively (bottom-left of Fig. 1A). The mean
151 relative abundance of the low latitude group (South) was significantly greater (by 1.84-
152 fold) than that of the high latitude group (North). In line with this, the α-diversity of
153 syntrophs, estimated based on OTU richness, significantly decreased with increasing
154 latitude (Fig. 1B). Having found this, we then identified the key environmental factors
155 related to the synTotal distribution through Spearman correlation analysis. Mean annual
156 temperature (MAT) and total soil sulfur (TS) were identified as the two most important
157 factors, followed by ammonium-nitrogen (NH_4^+-N), soil organic matter (OM), microbial
158 biomass carbon (MBC) and total nitrogen (TN) (Fig. 1C). Soil cation exchange capacity
159 (CEC) and pH showed negative correlations. The importance index estimated based on
160 the Boruta algorithm reiterated that MAT and TS were the two most important factors
161 linked to the biogeographical distribution of synTotal (Fig. 1C).

162 To compare the distribution of different syntrophs, the relative abundances of five
163 syntroph genera were individually analyzed (Fig. S3). The distributions of
164 *Syntrophobacter*, *Pelotomaculum*, *Smithella* and *Syntrophomonas* were consistent with
165 the distribution of the synTotal (Fig. S3A-D). *Desulfotomaculum* was an exception,
166 showing the highest abundance in the middle latitude regions (Fig. S3E). Division of the
167 low and high latitude groups revealed that the mean relative abundances of

For Peer Review Only

168 *Syntrophobacter*, *Syntrophomonas* and *Pelotomaculum* were significantly greater in the
169 low latitude regions than in the high latitude regions (Fig. S3F), in consistence with the
170 synTotal. *Syntrophobacter* had the highest mean relative abundance followed by
171 *Syntrophomonas* and *Smithella*, while *Pelotomaculum* and *Desulfotomaculum* showed
172 very low relative abundances (Fig. S3F).
173
174 **Biogeographical pattern of syntroph functioning potentials**
175 Next we evaluated the biogeographical pattern of syntroph functioning potentials.
176 For this purpose, fresh soil samples were incubated under anaerobic conditions at 30℃
177 with addition of 10 mM propionate. We tracked CH_4 production until >90% of the added
178 propionate had been consumed. Three distinct methane production patterns were
179 identified according to the time "lapse" required for CH_4 production from propionate
180 oxidation (Fig. 2). Pattern Ⅰ comprised 45 soil samples with a time lapse of 13 d to 27 d,
181 representing the high rate group of syntrophic metabolisms (Fig. 2A). The majority of
182 soil samples in this group was located at the low latitudes. Pattern Ⅱ, comprising 51
183 samples and representing the median rate of syntrophic metabolisms (28 d to 43 d) did
184 not show a distinct latitudinal tendency (Fig. 2B). The pattern Ⅲ group comprising 17
185 soil samples required 44 d to 82 d for CH_4 production from propionate oxidation and
186 hence represented the low rate group. The soils of this group were distributed mainly in
187 the cool high latitude regions (Fig. 2C). The SCFAs analyses further underpinned and
188 justified the separation of soil samples into three groups (Fig. 3A). Acetate was the major
189 intermediate detected in all samples (Fig. 3B). Butyrate was detected in 28.3% of soil
190 samples (detection limit of 0.05 mM) (Fig. 3C), most likely as an intermediate product

For Peer Review Only

from the C_6 dismutation pathway of *Smithella*. The highest butyrate concentrations occurred in the pattern Ⅲ soils (Fig. 3C). Taking all soil samples together, the time lapse for methanogenesis from propionate degradation displayed an explicit biogeographical pattern, being significantly slower in the high latitude soils than in the low latitude soils (Fig. 4A). Linear least squares regressions revealed that the time lapse for methanogenesis was significantly negatively correlated with the relative abundance of synTotal in original soils, MAT, TS, and other edaphic factors including soil OM, MBC, available Fe, Cu and Mn (Fig. 4C). The functional potential of propionate degradation can also be inferred from the maximum rate of methanogenesis (Fig. 4B), which supports the biogeographical tendency revealed by the time lapse.

Shifts in microbial community during anaerobic incubation with propionate

At the end of the anaerobic incubations, the structure of the microbial communities in the soil samples was revisited. The community composition at the phylum level did not show significant changes between the original soil samples and those after anaerobic incubations. The relative abundances of a few phyla, however, had changed markedly (Fig. S4A). Specifically, the relative abundances of *Proteobacteria* and *Acidobacteria* decreased during the incubations while those of *Actinobacteria*, *Firmicutes* and *Chloroflexi* were increased. As expected, the α-diversity of the bacterial communities at the OTU level showed a substantial decline at the end of the incubation compared with the original soils (Fig. S4B). The β-diversity at the genera level showed the separation of soil samples into two clusters for the low latitude and the high latitude soils, respectively (Fig. S4C). The co-occurrence network analysis of the top 10% OTUs confirmed that the

For Peer Review Only

OTUs for the low and high latitude regions tended to group separately (Fig. S4D). These results indicate that the bacterial community shifted significantly during anaerobic incubation, while the separation of metacommunities into the low latitude and the high latitude groups remained robust.

The relative abundance of syntrophs except *Desulfotomaculum* had increased markedly after the incubation with the maximum relative abundance of synTotal reaching 12.5%, indicating significant growth. We estimated the increase of individual syntrophs by calculating the logarithmic ($\log_2$) fold change (R) of the relative abundance before and after the incubation. The relative abundance of *Desulfotomaculum*, being low right at the beginning, did not change over the incubation (data not shown). The other four genera showed significant increases, but to different extents (Fig. 5). *Pelotomaculum* showed the greatest increase, followed by *Smithella* and *Syntrophomonas*, while *Syntrophobacter* exhibited the lowest increase (Fig. 5F). Strikingly, the relative increases of syntrophs showed an opposite geographic tendency compared with their relative abundances in the original soils (Fig. 2). The $\log_2$ R values for *Syntrophobacter*, *Syntrophomonas* and *Smithella* increased with the increase of latitude (Fig. 5A, B, D). The values for *Pelotomaculum* also increased with latitude, though showing the highest value at the middle latitude (Fig. 5C). These results indicate that the relative abundance of propionate syntrophs after anaerobic incubation increased to a greater extend in the high latitude soils compared to the low latitude soils.

Given their low relative abundances and their critical roles in oxidizing intermediate products during anaerobic decomposition of organic matter, propionate-oxidizing syntrophs represent a typical example of rare but important taxa in paddy soil microbiome. Here we show that the relative abundance of propionate syntrophs is

Wiley-Blackwell and Society for Applied Microbiology

For Peer Review Only

238 significantly correlated with MAT (Fig. 1). Based on the time lapse for propionate-fueled
239 methanogenesis, we further reveal that the biogeographical pattern of syntroph
240 functioning potentials (Figs. 2, 3) is in accordance with their relative abundances in soils.
241 It has been documented that within the physiological range, the microbial diversity,
242 metabolic activity and population growth rates in terrestrial ecosystems increase
243 exponentially with temperature (Zhou et al., 2016). Hence, climate warming is expected
244 to accelerate temporal turnover and divergent succession of microbial communities in
245 soils (Guo et al., 2018; Guo et al., 2019). In response to the increased temperature,
246 microbiota can also modulate metabolic and trophic interactions through shifting
247 functional guilds (Tveit et al., 2015). Syntrophs are known to have a specific lifestyle by
248 living at thermodynamic limit. Syntrophic propionate degradation has been revealed to be
249 temperature sensitive (Tveit et al., 2015). In order to obtain a deeper insight into the
250 temperature effect, we calculated the Gibbs free-energy changes ($\Delta G^{'}$) for the reaction of
251 propionate oxidation [$CH_3CH_2COO^-_{(aq)} + 2H_2O_{(l)} \rightarrow CH_3COO^-_{(aq)} + 3H_{2(g)} + CO_{2(g)}$] (Fig.
252 6A). ΔG^0_f and ΔH^0_f values for acetate and propionate were obtained from the database
253 established by Shock and Helgeson (Shock and Helgeson, 1990). We put temperature as
254 the only variable with other variables set to standard conditions and calculated the $\Delta G^{'}$ as
255 described by Hanselmann (Hanselmann, 1991). The calculated $\Delta G^{'}$ decreased linearly
256 with temperature at a rate of -0.44 kJ mol^{-1} $°C^{-1}$ (Fig. S5). Consequently, the cool high
257 latitude regions showed significantly higher positive values of $\Delta G^{'}$ than the warm low
258 latitude regions (Fig. 6A). The geographical distribution of the Gibbs free-energy changes
259 is in corroboration with the linear positive correlations of synTotal and the maximum rate
260 of CH_4 production with temperature (Fig. 6B,D) and with the negative correlation for the
261 time lapse of methanogenesis from propionate degradation (Fig. 6C). These correlations

For Peer Review Only

suggest that the decrease of Gibbs free-energy changes in the southern regions of China alleviates the thermodynamic tension, hence supporting the greater abundance and functional potential of propionate-oxidizing syntrophs compared with those in the northern regions. It has to be noted that the values of $\Delta G^{'}$ depicted in Fig. 6A are positive due to the use of standard conditions except temperature. In reality, negative $\Delta G^{'}$ values are to be expected due to low *in situ* concentrations of H_2 and acetate (Schutz et al., 1988; Kramer and Conrad, 1993). Fluctuations in concentrations of substrates and products actually can exert a significant impact on $\Delta G^{'}$, especially the fluctuations in H_2 as three moles of H_2 are produced per mole of propionate oxidized in the reaction mentioned above. Indeed, due to significant seasonal and spatial variations, the explanatory power of thermodynamics hinging on *in situ* concentrations of substrates and products has to be applied with care to infer geographical patterns at a large distance scale. Only very few studies have determined methanogenic substrates and products under quasi-steady conditions in paddy soil, which showed that H_2 concentrations were mostly lower than a few Pa (Schutz et al., 1988; Kramer and Conrad, 1993). Accumulation of such observations from different locations shall help shape a better understanding about geographical distributions of syntrophic organisms.

We found that the total sulfur content of the soil was the second most important factor influencing propionate syntroph biogeography. This was possibly due to the fact that many of propionate syntrophs, such as *Syntrophobacter fumaroxidans* and *Pelotomaculum thermopropionicum,* are facultative sulfate reducers (Harmsen et al., 1998; Imachi et al., 2002; Sedano-Nunez et al., 2018). In the presence of sulfate these organisms tend to perform anaerobic sulfate respiration instead of syntrophy with methanogens, maximizing energy conservation (Van Kuijk and Stams, 1995; Rebac et al.,

For Peer Review Only

1996; Worm et al., 2014; Li et al., 2018; Sedano-Nunez et al., 2018). Notably, while the relative abundances of *Syntrophobacter*, *Smithella* and *Syntrophomonas* in paddy soils were significantly correlated with TS, that of *Pelotomaculum* was not (Fig. 1C). Therefore, individual syntrophs have different responses to TS. Besides TS, the relative abundances of syntrophs were also positively correlated with the contents of soil OM, total N, MBC; additionally the functioning potential was correlated with the contents of trace elements Fe, Cu and Mn (Fig. 4C). Since a high soil OM content is usually associated with high TN, MBC and trace element contents and even TS, these edaphic factors are probably co-variables, yet the positive correlations likely indicate the favorable living conditions for most microbes including syntrophs.

Anaerobic incubation with propionate caused a marked shift in the soil bacterial community (Fig. S4). Specifically, the relative abundances of syntrophic populations increased by up to 29-fold over the incubation period. The increase in relative abundances, however, differed among the five syntroph genera. *Pelotomaculum* showed the greatest growth, followed by *Smithella* and *Syntrophomonas* while *Syntrophobacter* and *Desulfotomaculum* grew the least (Fig. 5). These results indicate that *Pelotomaculum* species have the most potential to be active in paddy soils across a wide range of geographical locations when favorable conditions become available. *Smithella* in combination with *Syntrophomonas* are the next group with high metabolic potentials, while *Desulfotomaculum* showed virtually no response. Compared to the other three syntroph genera (*Pelotomaculum*, *Smithella* and *Syntrophomonas*), *Syntrophobacter* had the highest mean relative abundance in original soils (Fig. S3) but showed the least increase after the incubation (Fig. 5). Probably, under a warmer 30℃ condition during the incubation (compared with the mean summer temperature of 17-29℃ across sampling

Wiley-Blackwell and Society for Applied Microbiology

For Peer Review Only

310 sites), *Syntrophobacter* were less competitive in utilizing propionate than the other
311 syntrophs (Gan et al., 2012; Chen et al., 2020). Alternately, it is also likely that
312 *Pelotomaculum* and *Smithella* reacted faster than *Syntrophobacter* when an adequate
313 concentration of propionate (10 mM in this study) was supplied. *Pelotomaculum* and
314 *Smithella* are known to use the methylmalonyl-CoA (MMC) pathway and the C_6
315 dismutation pathway, respectively (Liu et al., 1999; de Bok et al., 2001; Mueller et al.,
316 2010; Xia et al., 2019). Due to the necessity of only two electrons released from the C_6
317 pathway compared with six electrons from the MMC pathway per propionate oxidized,
318 *Smithella* are considered to have a larger window of opportunity in environments than the
319 MMC-utilizing syntrophs (Dolfing, 2013). The calculation of $\Delta G'$ values indicates that
320 the energetics of the C_6 pathway is less sensitive to temperature than the MMC pathway
321 (Fig. S6). Consistent with this, we found that the maximum increase of relative
322 abundance occurred at the middle latitudes for *Pelotomaculum* but farther north for
323 *Smithella* and *Syntrophomonas* (Fig. 5A vs B and D). Together with the detection of
324 butyrate as a significant intermediate (Fig. 3C), our results suggest that *Smithella* and
325 *Syntrophomonas* likely form syntrophic interaction during propionate degradation and
326 they are potentially more active in the cool high latitude soils.
327 The increase in relative abundances, expressed as $\log_2 R$, tended to be greater in the
328 high latitude soils relative to the low latitude soils (Fig. 5), in contrast to the geographical
329 distribution of relative abundances in original soils (Fig. 1). There are three plausible
330 explanations for this result. Firstly, in a mixed community, not only syntrophs are present
331 (Fig. S4), and a relatively slow response of those other organisms would result in a
332 relative increase of syntrophs. Secondly, for an initially low biomass (which appears to be
333 the case in the present experiment), consumption of an identical quantity of substrate is

For Peer Review Only

expected to produce a greater fold change of biomass compared with a group of organisms having an initial high biomass. Thirdly, the anaerobic incubations were stopped when >90% of propionate were consumed, which resulting in incubations of between 13 d and 82 d for different soils (Fig. 2). A longer duration may have resulted in a greater biomass yield per unit substrate consumption by preventing energetic loss from overflow metabolism (e.g. futile cycles and protein synthesis) (Thauer et al., 2008; Beardmore et al., 2011; Lipson, 2015; Seel et al., 2016). Whether this rate-yield tradeoff relationship really exists in paddy soil syntrophs requires further investigation.

In summary, we demonstrate in the present study that both the relative abundance and functioning potential of propionate syntrophs in paddy field soils exhibit a distinct biogeographical pattern. MAT and TS are identified as the two most important factors related to the biogeographical distribution. The temperature effect is very likely related to thermodynamic conditions, which improve when the temperature increases. The effect of soil sulfur content is possibly due to the fact that some facultative propionate syntrophs perform sulfate respiration in the presence of sulfate. Though originating from areas with a MAT lower by only 6.7℃, the mean time lapse for methanogenesis from propionate degradation was approximately 30 d longer in the high latitude soils relative to the low latitude soils. This result, on the one hand, indicates that the rates of organic matter decomposition and C cycling are potentially lower in the cool high latitude regions. On the other hand, it suggests that the global warming, which is occurring to a greater extent at the high latitudes, can cause a significant acceleration of organic matter decomposition and C cycling in the high latitude soils.

Data availability

For Peer Review Only

The datasets supporting the conclusions of this article are available in the NCBI Sequence Read Archive under BioProject PRJNA544819 and PRJNA601098 that are publicly accessible at https://www.ncbi.nlm.nih.gov. R codes on the statistical analyses are available at https://github.com/jinyidan/Rare-Biosphere-Propionate-Syntrophs-in-Paddy-Field-Soils.

Acknowledgments

This work was made possible through two NSFC (National Natural Science Foundation of China) grants (91951206, 41630857) and a grant from National Basic Research Program of China (2016YFD0200306).

Y.L., S.J., Y.J. designed the study. S.J. conducted field soil sampling. Y.J. and S.J. executed lab work. Y.J., S.J. and Y.L. analyzed the data. J.D. helped perform the data analysis with constructive discussions. Y.L. and Y.J. wrote the original manuscript. All authors read, revised and approved the final manuscript.

The authors declare that they have no competing interests.

References

Bahram, M., Hildebrand, F., Forslund, S.K., Anderson, J.L., Soudzilovskaia, N.A., Bodegom, P.M. et al. (2018) Structure and function of the global topsoil microbiome. *Nature* **560**: 233-237.

Beardmore, R.E., Gudelj, I., Lipson, D.A., and Hurst, L.D. (2011) Metabolic trade-offs and the maintenance of the fittest and the flattest. *Nature* **472**: 342-346.

Boe, K., Batstone, D.J., Steyer, J.-P., and Angelidaki, I. (2010) State indicators for monitoring the anaerobic digestion process. *Water Res* **44**: 5973-5980.

For Peer Review Only

382 Chen, Y.T., Zeng, Y., Wang, H.Z., Zheng, D., Kamagata, Y., Narihiro, T. et al. (2020)
383 Different interspecies electron transfer patterns during mesophilic and thermophilic
384 syntrophic propionate degradation in chemostats. *Microb Ecol* **80**: 120-132.
385 Conrad, R. (2009) The global methane cycle: recent advances in understanding the
386 microbial processes involved. *Environ Microbiol Rep* **1**: 285-292.
387 Crowther, T.W., van den Hoogen, J., Wan, J., Mayes, M.A., Keiser, A.D., Mo, L. et al.
388 (2019) The global soil community and its influence on biogeochemistry. *Science* **365**:
389 eaav0550.
390 de Bok, F.A.M., Stams, A.J.M., Dijkema, C., and Boone, D.R. (2001) Pathway of
391 propionate oxidation by a syntrophic culture of *Smithella propionica* and
392 *Methanospirillum hungatei*. *Appl Environ Microbiol* **67**: 1800-1804.
393 Delgado-Baquerizo, M., Oliverio, A.M., Brewer, T.E., Benavent-Gonzalez, A., Eldridge,
394 D.J., Bardgett, R.D. et al. (2018) A global atlas of the dominant bacteria found in soil.
395 *Science* **359**: 320-325.
396 Deng, N., Grassini, P., Yang, H., Huang, J., Cassman, K.G., and Peng, S. (2019) Closing
397 yield gaps for rice self-sufficiency in China. *Nat Commun* **10**: 1725.
398 Dolfing, J. (2013) Syntrophic propionate oxidation via butyrate: a novel window of
399 opportunity under methanogenic conditions. *Appl Environ Microbiol* **79**: 4515-4516.
400 Dyksma, S., and Gallert, C. (2019) *Candidatus* Syntrophosphaera thermopropionivorans:
401 a novel player in syntrophic propionate oxidation during anaerobic digestion. *Environ*
402 *Microbiol Rep* **11**: 558-570.
403 Gan, Y., Qiu, Q., Liu, P., Rui, J., and Lu, Y. (2012) Syntrophic oxidation of propionate in
404 rice field soil at 15 and 30°C under methanogenic conditions. *Appl Environ Microbiol* **78**:
405 4923-4932.

For Peer Review Only

406 Garbeva, P., van Veen, J.A., and van Elsas, J.D. (2004) Microbial diversity in soil:
407 selection of microbial populations by plant and soil type and implications for disease
408 suppressiveness. *Annu Rev Phytopathol* **42**: 243-270.
409 Glissmann, K., and Conrad, R. (2000) Fermentation pattern of methanogenic degradation
410 of rice straw in anoxic paddy soil. *FEMS Microbiol Ecol* **31**: 117-126.
411 Glissmann, K., Weber, S., and Conrad, R. (2001) Localization of processes involved in
412 methanogenic in degradation of rice straw in anoxic paddy soil. *Environ Microbiol* **3**:
413 502-511.
414 Guo, X., Feng, J., Shi, Z., Zhou, X., Yuan, M., Tao, X. et al. (2018) Climate warming
415 leads to divergent succession of grassland microbial communities. *Nat Clim Change* **8**:
416 813-818.
417 Guo, X., Zhou, X., Hale, L., Yuan, M., Ning, D., Feng, J. et al. (2019) Climate warming
418 accelerates temporal scaling of grassland soil microbial biodiversity. *Nat Ecol Evol* **3**:
419 612-619.
420 Haefele, S.M., Nelson, A., and Hijmans, R.J. (2014) Soil quality and constraints in global
421 rice production. *Geoderma* **235**: 250-259.
422 Hanselmann, K.W. (1991) Microbial energetics applied to waste repositories. *Experientia*
423 **47**: 645-687.
424 Harmsen, H.J.M., Van Kuijk, B.L.M., Plugge, C.M., Akkermans, A.D.L., De Vos, W.M.,
425 and Stams, A.J.M. (1998) *Syntrophobacter fumaroxidans* sp. nov., a syntrophic
426 propionate-degrading sulfate-reducing bacterium. *Int J Syst Bacteriol* **48**: 1383-1387.
427 Hidalgo-Ahumada, C.A.P., Nobu, M.K., Narihiro, T., Tamaki, H., Liu, W.-T., Kamagata,
428 Y. et al. (2018) Novel energy conservation strategies and behaviour of *Pelotomaculum*
429 *schinkii* driving syntrophic propionate catabolism. *Environ Microbiol* **20**: 4503-4511.

Wiley-Blackwell and Society for Applied Microbiology

For Peer Review Only

Imachi, H., Sekiguchi, Y., Kamagata, Y., Hanada, S., Ohashi, A., and Harada, H. (2002) *Pelotomaculum thermopropionicum* gen. nov., sp nov., an anaerobic, thermophilic, syntrophic propionate-oxidizing bacterium. *Int J Syst Evol Microbiol* **52**: 1729-1735.

Imachi, H., Sakai, S., Ohashi, A., Harada, H., Hanada, S., Kamagata, Y., and Sekiguchi, Y. (2007) *Pelotomaculum propionicicum* sp nov., an anaerobic, mesophilic, obligately syntrophic propionate-oxidizing bacterium. *Int J Syst Evol Microbiol* **57**: 1487-1492.

Imachi, H., Sekiguchi, Y., Kamagata, Y., Loy, A., Qiu, Y.L., Hugenholtz, P. et al. (2006) Non-sulfate-reducing, syntrophic bacteria affiliated with *Desulfotomaculum* cluster I are widely distributed in methanogenic environments. *Appl Environ Microbiol* **72**: 2080-2091.

Kramer, H., and Conrad, R. (1993) Measurement of dissolved H_2 concentrations in methanogenic environments with a gas-siffusion probe. *FEMS Microbiol Ecol* **12**: 149-158.

Krylova, N.I., Janssen, P.H., and Conrad, R. (1997) Turnover of propionate in methanogenic paddy soil. *FEMS Microbiol Ecol* **23**: 107-117.

Li, H.J., Chang, J.L., Liu, P.F., Fu, L., Ding, D.W., and Lu, Y.H. (2015) Direct interspecies electron transfer accelerates syntrophic oxidation of butyrate in paddy soil enrichments. *Environ Microbiol* **17**: 1533-1547.

Li, Y., Sun, Y., Li, L., and Yuan, Z. (2018) Acclimation of acid-tolerant methanogenic propionate-utilizing culture and microbial community dissecting. *Bioresour Technol* **250**: 117-123.

Lipson, D.A. (2015) The complex relationship between microbial growth rate and yield and its implications for ecosystem processes. *Front Microbiol* **6**: 615.

Liu, Y.T., Balkwill, D.L., Aldrich, H.C., Drake, G.R., and Boone, D.R. (1999) Characterization of the anaerobic propioate-degrading syntrophs *Smithella propionica*

For Peer Review Only

gen. nov., sp. nov. and *Syntrophobacter wolinii*. *Int J Syst Bacteriol* **49**: 545-556.

Lueders, T., Pommerenke, B., and Friedrich, M.W. (2004) Stable-isotope probing of microorganisms thriving at thermodynamic limits: syntrophic propionate oxidation in flooded soil. *Appl Environ Microbiol* **70**: 5778-5786.

Lynch, M.D., and Neufeld, J.D. (2015) Ecology and exploration of the rare biosphere. *Nat Rev Microbiol* **13**: 217-229.

McInerney, M.J., Sieber, J.R., and Gunsalus, R.P. (2009) Syntrophy in anaerobic global carbon cycles. *Curr Opin Biotechnol* **20**: 623-632.

Mueller, N., Worm, P., Schink, B., Stams, A.J.M., and Plugge, C.M. (2010) Syntrophic butyrate and propionate oxidation processes: from genomes to reaction mechanisms. *Environ Microbiol Rep* **2**: 489-499.

Nilsen, R.K., Torsvik, T., and Lien, T. (1996) *Desulfotomaculum thermocisternum* sp nov, a sulfate reducer isolated from a hot North Sea oil reservoir. *Int J Syst Bacteriol* **46**: 397-402.

Noll, M., Klose, M., and Conrad, R. (2010) Effect of temperature change on the composition of the bacterial and archaeal community potentially involved in the turnover of acetate and propionate in methanogenic rice field soil. *FEMS Microbiol Ecol* **73**: 215-225.

Peng, J., Wegner, C.-E., Bei, Q., Liu, P., and Liesack, W. (2018) Metatranscriptomics reveals a differential temperature effect on the structural and functional organization of the anaerobic food web in rice field soil. *Microbiome* **6**: 169.

Plugge, C.M., Balk, M., and Stams, A.J.M. (2002) *Desulfotomaculum thermobenzoicum* subsp *thermosyntrophicum* subsp nov., a thermophilic, syntrophic, propionate-oxidizing, spore-forming bacterium. *Int J Syst Evol Microbiol* **52**: 391-399.

Wiley-Blackwell and Society for Applied Microbiology

For Peer Review Only

Qi, W., Liu, S.H., Zhao, M.F., and Liu, Z. (2016) China's different spatial patterns of population growth based on the "Hu Line". *J Geogr Sci* **26**: 1611-1625.

Rebac, S., Visser, A., Gerbens, S., VanLier, J.B., Stams, A.J.M., and Lettinga, G. (1996) The effect of sulphate on propionate and butyrate degradation in a psychrophilic anaerobic expanded granular sludge bed (EGSB) reactor. *Environ Technol* **17**: 997-1005.

Rillig, M.C., Ryo, M., Lehmann, A., Aguilar-Trigueros, C.A., Buchert, S., Wulf, A. et al. (2019) The role of multiple global change factors in driving soil functions and microbial biodiversity. *Science* **366**: 886-890.

Rui, J., Peng, J., and Lu, Y. (2009) Succession of bacterial populations during plant residue decomposition in rice field soil. *Appl Environ Microbiol* **75**: 4879-4886.

Schink, B. (1997) Energetics of syntrophic cooperation in methanogenic degradation. *Microbiol Mol Biol Rev* **61**: 262-280.

Schink, B., and Stams, A.J.M. (2006) Syntrophism among prokaryotes. In *The Prokaryotes*. Dworkin, M., Falkow, S., Rosenberg, E., Schleifer, K.H., and Stackebrandt, E. (eds). New York: Springer, pp. 309-335.

Schlatter, D.C., Bakker, M.G., Bradeen, J.M., and Kinkel, L.L. (2015) Plant community richness and microbial interactions structure bacterial communities in soil. *Ecology* **96**: 134-142.

Schutz, H., Conrad, R., Goodwin, S., and Seiler, W. (1988) Emission of hydrogen from feep and dhallow fresh-water environments. *Biogeochemistry* **5**: 295-311.

Sedano-Nunez, V.T., Boeren, S., Stams, A.J.M., and Plugger, C.M. (2018) Comparative proteome analysis of propionate degradation by *Syntrophobacter fumaroxidans* in pure culture and in coculture with methanogens. *Environ Microbiol* **20**: 1842-1856.

Seel, W., Derichs, J., and Lipski, A. (2016) Increased biomass production by mesophilic

For Peer Review Only

food-associated bacteria through lowering the growth temperature from 30°C to 10°C. *Appl Environ Microbiol* **82**: 3754-3764.

Shock, E.L., and Helgeson, H.C. (1990) Calculation of the thermodynamic and transport-properties of aqueous species at high-pressures and temperatures: standard partial molal properties of organic-species. *Geochim Cosmochim Acta* **54**: 915-945.

Sieber, J.R., McInerney, M.J., and Gunsalus, R.P. (2012) Genomic insights into syntrophy: the paradigm for anaerobic metabolic cooperation. *Annu Rev Microbiol* **66**: 429-452.

Singh, A., Schnurer, A., and Westerholm, M. (2021) Enrichment and description of novel bacteria performing syntrophic propionate oxidation at high ammonia level. *Environ Microbiol*: doi:10.1111/1462-2920.15388.

Stams, A.J., and Plugge, C.M. (2009) Electron transfer in syntrophic communities of anaerobic bacteria and archaea. *Nat Rev Microbiol* **7**: 568-577.

Steidinger, B.S., Crowther, T.W., Liang, J., Van Nuland, M.E., Werner, G.D.A., Reich, P.B. et al. (2019) Climatic controls of decomposition drive the global biogeography of forest-tree symbioses. *Nature* **569**: 404-408.

Thauer, R.K. (1998) Biochemistry of methanogenesis: a tribute to Marjory Stephenson. *Microbiology* **144**: 2377-2406.

Thauer, R.K., Kaster, A.K., Seedorf, H., Buckel, W., and Hedderich, R. (2008) Methanogenic archaea: ecologically relevant differences in energy conservation. *Nat Rev Microbiol* **6**: 579-591.

Tveit, A.T., Urich, T., Frenzel, P., and Svenning, M.M. (2015) Metabolic and trophic interactions modulate methane production by Arctic peat microbiota in response to warming. *Proc Natl Acad Sci U S A* **112**: E2507-E2516.

For Peer Review Only

van den Hoogen, J., Geisen, S., Routh, D., Ferris, H., Traunspurger, W., Wardle, D.A. et al. (2019) Soil nematode abundance and functional group composition at a global scale. *Nature* **572**: 194-198.

Van Kuijk, B.L., and Stams, A.J. (1995) Sulfate reduction by a syntrophic propionate-oxidizing bacterium. *Anton Leeuw Int J G* **68**: 293-296.

Worm, P., Koehorst, J.J., Visser, M., Sedano-Nunez, V.T., Schaap, P.J., Plugge, C.M. et al. (2014) A genomic view on syntrophic versus non-syntrophic lifestyle in anaerobic fatty acid degrading communities. *Biochim Biophys Acta* **1837**: 2004-2016.

Xia, X., Zhang, J., Song, T., and Lu, Y. (2019) Stimulation of *Smithella*-dominating propionate oxidation in a sediment enrichment by magnetite and carbon nanotubes. *Environ Microbiol Rep* **11**: 236-248.

Zhang, C.Y., Liu, X.L., and Dong, X.Z. (2004) *Syntrophomonas curvata* sp nov., an anaerobe that degrades fatty acids in co-culture with methanogens. *Int J Syst Evol Microbiol* **54**: 969-973.

Zhou, J., Deng, Y., Shen, L., Wen, C., Yan, Q., Ning, D. et al. (2016) Temperature mediates continental-scale diversity of microbes in forest soils. *Nat Commun* **7**: 12083.

Figure Legends

Figure 1: Biogeographic distribution of propionate syntrophs in paddy field soils across eastern China. (A) The map shows the spatial distribution of total relative abundance (Rel. abun.) of five syntroph genera (referred to synTotal) comprising *Syntrophobacter*, *Pelotomaculum*, *Smithella*, *Desulfotomaculum* and *Syntrophomonas* together. The map was built using Kriging interpolation method with cross-validation (cv) based on Pearson

Wiley-Blackwell and Society for Applied Microbiology

For Peer Review Only

correlation. The inset in lower-left corner shows the difference in mean relative abundance of synTotal between the low (South) and the high (North) latitude soils. The red asterisks indicate the significant difference at $P \leq 0.001$. (B) The α-diversity of propionate syntrophs expressed as OTU richness, which decreases with the increase of latitude. The solid line denotes the least-squares linear regression, which was significant at $P < 0.0001$. (C) Correlations between the relative abundance of propionate syntrophs (either in total or individually) and environmental factors. The color and size of circles indicate the Spearman correlation coefficients. The black asterisks indicate the significant correlations: * $0.01 < P \leq 0.05$, ** $0.001 < P \leq 0.01$, *** $P \leq 0.001$. Bars in the right show the importance of environmental factors to five syntroph genera estimated based on Boruta algorithm. The environmental factors include the mean annual temperature (MAT) and fifteen edaphic factors: the content of soil organic matter (OM), dissolved organic carbon (DOC), pH, cation exchange capacity (CEC), microbial biomass carbon (MBC), the total contents of N, P, K, S, Fe, Mn, Cu, Zn (TN, TP, TK, TS, TFe, TMn, TCu, TZn), ammonium (NH_4^+) and nitrate (NO_3^-).

Figure 2: Geographic features of CH_4 production from propionate degradation in paddy field soils. The time till CH_4 production reached the quantity corresponding to >90% degradation of propionate added was defined as the time lapse. Three patterns can be distinguished from 113 paddy field soils analyzed. (A) Pattern Ⅰ, representing the high rate group, comprises 45 soil samples (red dots), having time lapses of 13 d to 27 d. (B) Pattern Ⅱ, representing the medium rate group, includes 51 soil samples (green dots), with time lapses of 28 d to 43 d. (C) Pattern Ⅲ, the low rate group, contains 17 soil

For Peer Review Only

samples (blue dots), having the time lapse of 44 d to 82 d. The CH_4 production curves of each soil in the three groups are illustrated in the lower-left corner of each panel. The CH_4 production curves within each group are colored randomly; the two vertical grey dot lines denote the ranges of time lapse. The error bars indicate the standard deviation of three replicates. All soil samples are displayed in maps with the pattern-specific samples highlighted by the increased sizes of the colored dots (red for Pattern Ⅰ, green for Pattern Ⅱ and blue for Pattern Ⅲ).

Figure 3: The dynamics of short-chain fatty acids in paddy soils during anaerobic incubation. Propionate was added to a final concentration of 10 mM to each soil samples, which were incubated anaerobically until at least >90% of propionate had been oxidized. (A) The consumption of propionate. (B and C) The transient accumulations of acetate and butyrate, respectively. Soil samples are separated into three groups in accordance with three patterns revealed by methanogenesis, circles for Pattern Ⅰ, triangles for Pattern ⅠⅡ and diamonds for Pattern Ⅲ. Soil samples within each group are colored randomly.

Figure 4: Geographical distribution of syntrophic potential and the correlative factors. (A) The map showing the functioning potential expressed as the time lapse for propionate degradation. The shorter the time lapse, the higher the functioning potential. (B) The map showing the functioning potential expressed as the maximum rate of CH_4 production, which was estimated during the period when CH_4 concentration was at the linear increase. The maps in (A) and (B) were build using Kriging interpolation method. The insets in the lower-left corner of each panel display the actual values of the time lapse (blue) and the

For Peer Review Only

maximum rate (red) of CH_4 production, respectively. (C) The correlations of the time lapse with the relative abundance of total syntrophs (Rel. abun. of synTotal), the mean annual temperature (MAT), the contents of total soil sulfur (TS), organic matter (OM), microbial biomass carbon (MBC), and the bioavailable contents of Fe, Cu and Mn (AFe, ACu, AMn). The solid lines denote the least-squares linear regressions. Individual soil samples are colored from blue to red in correspondence with their locations from the low latitudes to the high latitudes.

Figure 5: The relative growth of propionate syntrophs during anaerobic incubation. The relative growth was expressed as the logarithmic (log_2) fold change (R) in relative abundance of individual syntroph genera over the anaerobic incubation. (A-D) The geographic distributions of relative growth of *Syntrophobacter*, *Syntrophomonas*, *Pelotomaculum* and *Smithella*, respectively. (E) The mean relative abundances of four syntroph genera at the end of the anaerobic incubation. (F) The mean log_2 fold change (R) in relative abundance of four syntroph genera. Soil samples in (E) and (F) were clustered into two geographic groups for the low latitude regions (South) and the high latitude regions (North), respectively. The red asterisks denote the significant differences between the "South" and "North" groups: * $0.01 < P \leq 0.05$, ** $P \leq 0.01$.

Figure 6: The geographical features of Gibbs free-energy changes for propionate degradation. (A) The geographic distribution of Gibbs free-energy changes ($\Delta G'$) for propionate oxidation corrected by temperature. The mean summer temperature (from June to September) at sampling sites was used to correct the calculation of Gibbs free-energy changes for the reaction: $CH_3CH_2COO^-_{(aq)} + 2H_2O_{(l)} \rightarrow CH_3COO^-_{(aq)} + 3H_{2(g)} +$

For Peer Review Only

620 $CO_{2(g)}$. The values of standard Gibbs free-energy changes (ΔG^0) and enthalpy changes
621 (ΔH^0) at 25℃ (i.e. 298.15 K, 100 kPa, 1 M) equal to +73.5 kJ and +205.1 kJ per mol of
622 propionate, respectively (for calculation details, see the Supplemental Material). The inset
623 in the lower-left corner shows the difference in mean ΔG between two geographic groups
624 for the low (South) and the high (North) latitude soils, respectively. The red asterisks
625 indicate the significant difference at $P \leq 0.001$. (B) The correlation of synTotal relative
626 abundance with temperature. (C) The correlation of time lapse for propionate degradation
627 with temperature. (D) The correlation of maximum rate of CH_4 production with
628 temperature. The solid lines in (B-D) denote the least-squares linear regressions.
629 Individual soil samples are colored from blue to red in correspondence with their
630 locations from the low latitudes to the high latitudes.
631
632 **Supporting Information**
633 **Figure S1.** Phylogenetic relationship of 528 dominant OTUs (top 2.5%) retrieved from
634 113 paddy field soils. **Figure S2.** Neighbor-joining tree of 16S rRNA gene sequences
635 related to five syntroph genera including representative sequences retrieved from this
636 study and the reference sequences. **Figure S3.** Biogeographical distributions of five
637 syntroph genera in paddy field soils across eastern China. **Figure S4.** Bacterial
638 community in original soils and in soil samples after anaerobic incubations. **Figure S5.**
639 The effect of temperature on the Gibbs free energy change of propionate oxidation via the
640 methylmalonyl-CoA pathway. **Figure S6.** Temperature sensitivity of the Gibbs free
641 energy changes of propionate oxidation through the methylmalonyl-CoA pathway vs the
642 C_6 dismutation pathway. (PDF 2511 kb)

For Peer Review Only

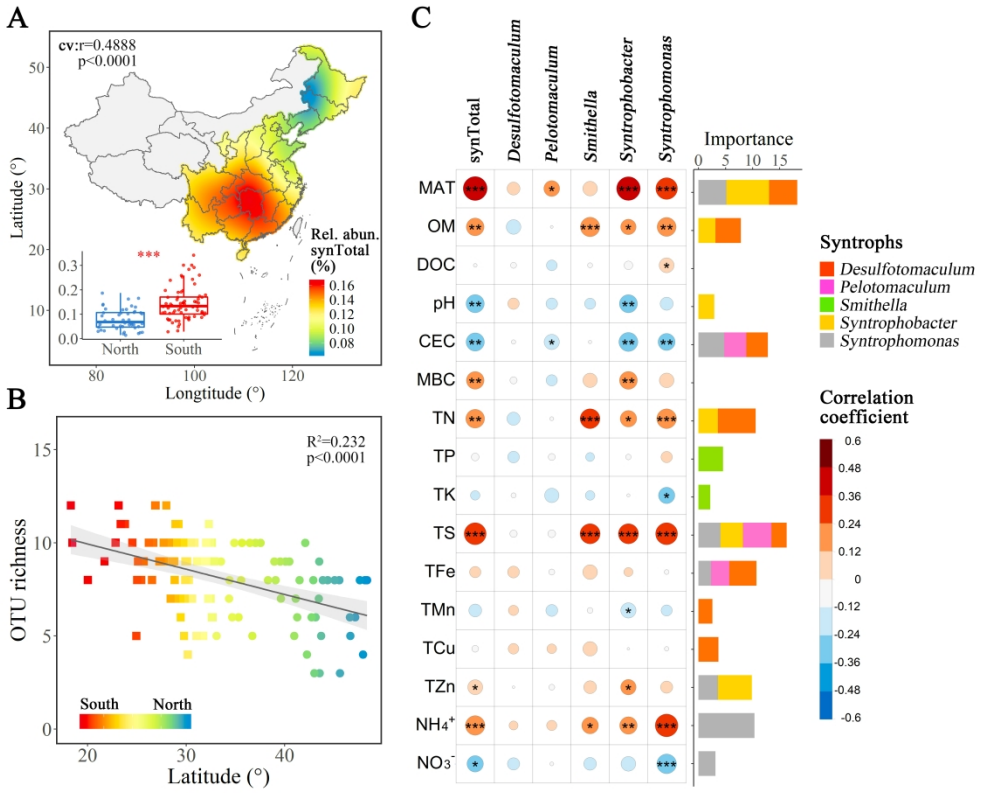

Figure 1: Biogeographic distribution of propionate syntrophs in paddy field soils across eastern China.

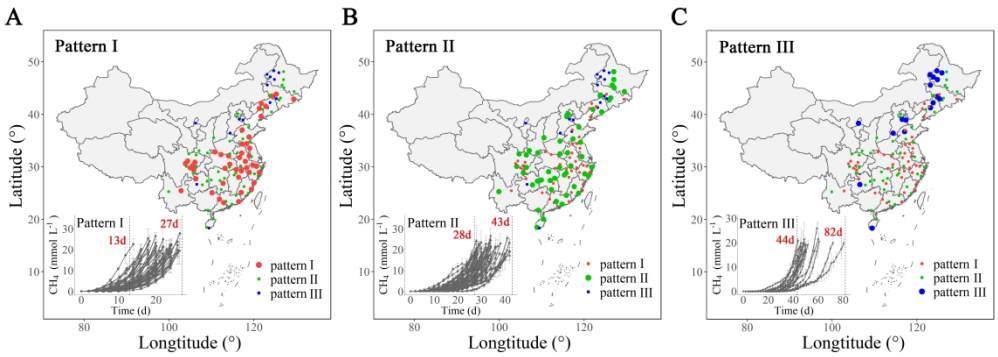

Figure 2: Geographic features of CH4 production from propionate degradation in paddy field soils.

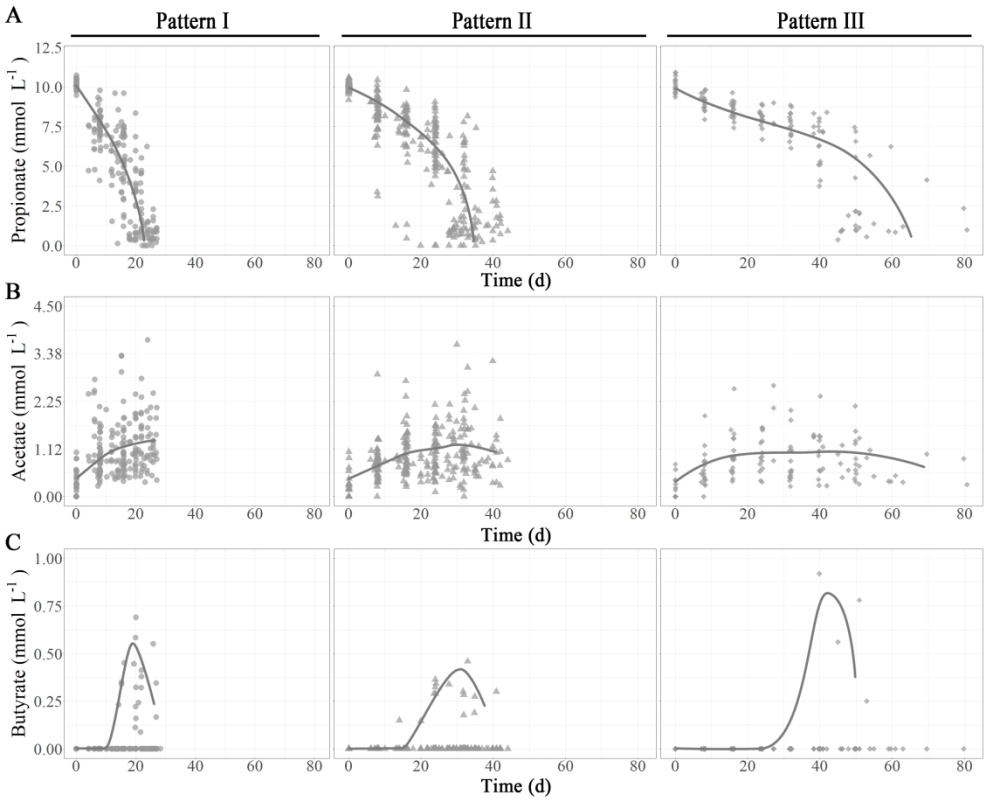

Figure 3: The dynamics of short-chain fatty acids in paddy soils during anaerobic incubation.

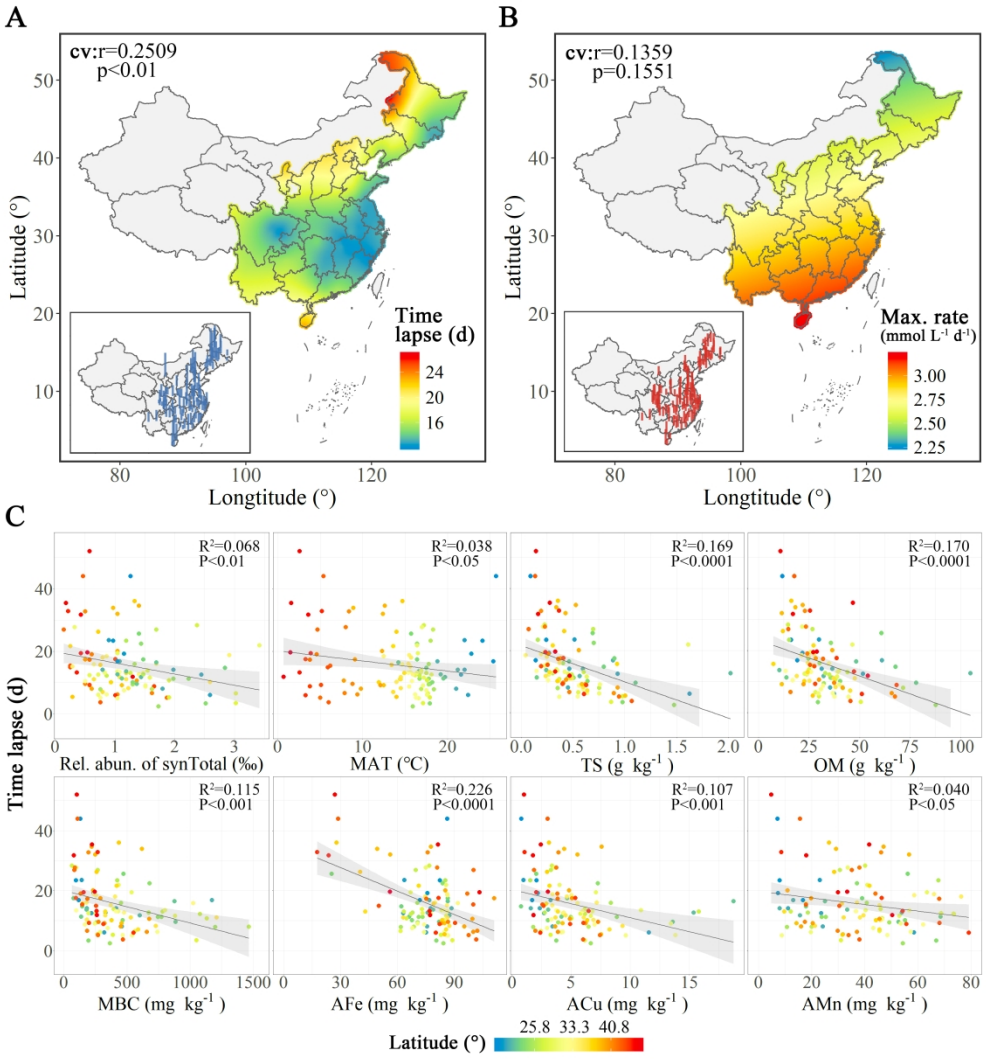

Figure 4: Geographical distribution of syntrophic potential and the correlative factors.

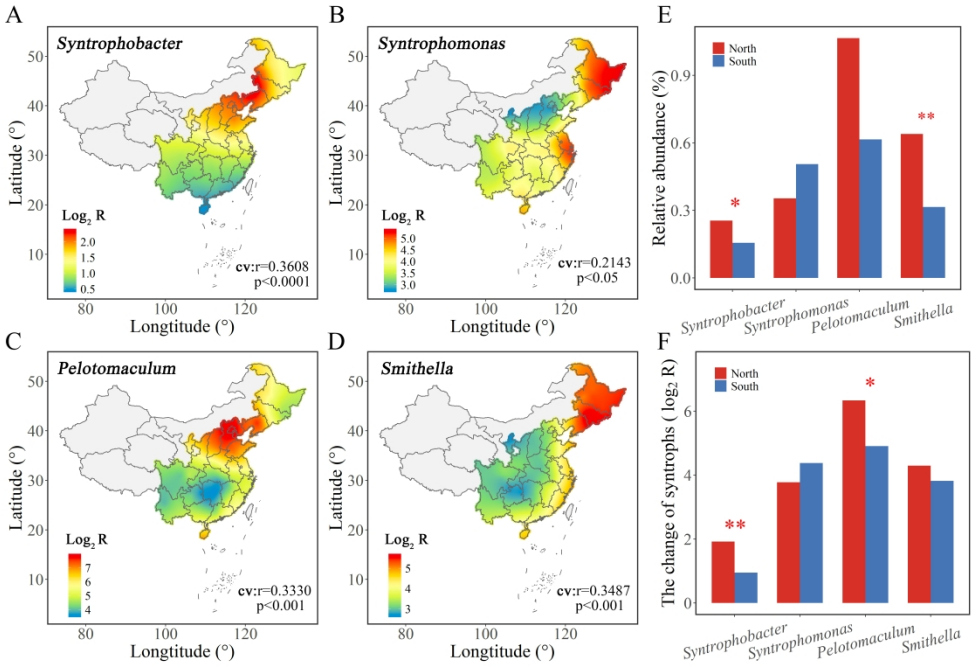

Figure 5: The relative growth of propionate syntrophs during anaerobic incubation.

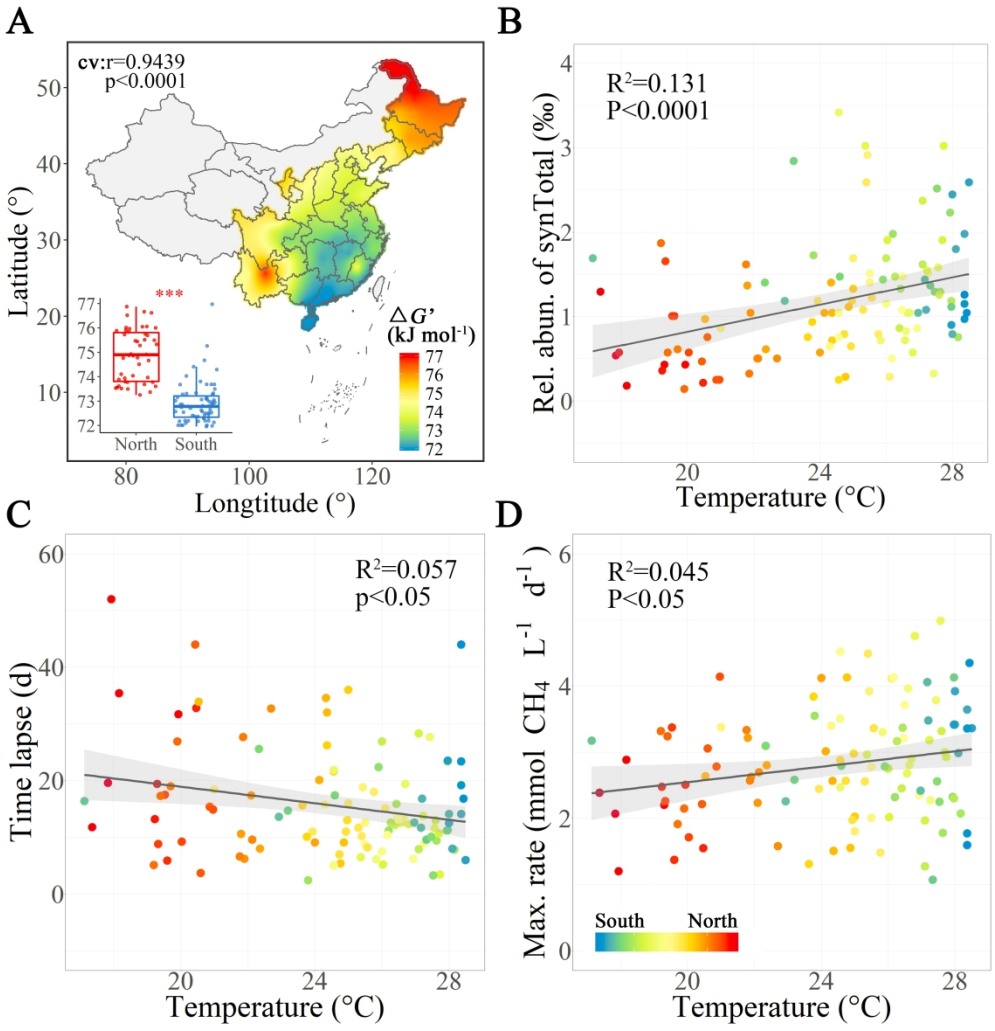

Figure 6: The geographical features of Gibbs free-energy changes for propionate degradation.